ELSEVIER

Thermochimica Acta 397 (2003) 55–66

thermochimica acta

www.elsevier.com/locate/tca

Thermodynamic study of the solid–liquid equilibria in the M^IPO_3–$Ce(PO_3)_3$ systems (M^I = Li, Na, K, Rb, Cs, Ag, Tl)

Chokri Marhag [a], Dalila Ben Hassen-Chehimi [b], Hechmi Said [a,*]

[a] *Laboratoire de Thermodynamique, Département de Chimie Faculté des Sciences de Bizerte,*
7021 Zarzouna-Bizerte, Tunisia
[b] *Laboratoire de Physico-Chimie Minérale, Faculté des Sciences de Bizerte,*
7021 Zarzouna-Bizerte, Tunisia

Received 29 November 2001; received in revised form 22 April 2002; accepted 29 April 2002

Abstract

An equation of the liquidus curve of a stoichiometric phase has been established in a previous publication. In this work, the obtained formula is applied to the phase diagram determination of the M^IPO_3–$Ce(PO_3)_3$ (with M^I = Li, Na, K, Rb, Cs, Ag, Tl) systems. The temperature, enthalpy and entropy of fusion are calculated for each solid phase with the exception of lithium and silver polyphosphates, of which crystallization fields were very limited. The enthalpy of fusion of all of these polyphosphates is determined from the DTA curves. The melting enthalpy of $Ce(PO_3)_3$, calculated from different binary systems is approximately equal to the measured value. The calculated temperatures and compositions are in good agreement with experimental determinations.

Keywords: Phase diagram; Binary system; Polyphosphates; Enthalpy; DTA

1. Introduction

The experimental study, the graphical representation, the exploitation of phase diagrams or the critical evaluation of experimental values, involve convenient models. The coherence of these models with thermodynamical constraints must always be checked. It prevents erroneous representation of phase equilibria and allows a better understanding and interpretation of experiments or the calculation of significant thermodynamical data.

Analysis, processing and thermodynamic exploitation of solid–liquid equilibria curves of M^IPO_3–$Ce(PO_3)_3$ systems (with M^I = Li, Na, K, Rb, Cs, Ag, Tl) are presented in this paper. Phase diagrams of corresponding systems have been established previously [1]. This study showed the existence of two intermediate compounds: $M^ICe(PO_3)_4$, $M^I_2Ce(PO_3)_5$ with M^I = K, Rb, Cs, Tl and only one compound $M^ICe(PO_3)_4$ with M^I = Li, Na, Ag. All compounds decomposed peritectically upon heating.

In order to refine and to interpret the experimental data, we have applied to these systems a semi-empirical equation [2–4] already used with success for similar binary systems, and many water–salt binary systems.

A complementary study using calorimetry was undertaken to control thermodynamic values of monovalent metal polyphosphates [4] and cerium polyphosphate, determined by liquidus curve computation.

---

* Corresponding author. Tel.: +216-72-591-906;
fax: +216-72-590-566.
E-mail address: chokri.marhag@fsb.rnu.tn (C. Marhag).

0040-6031/02/$ – see front matter © 2002 Elsevier Science B.V. All rights reserved.
PII: S0040-6031(02)00315-5

Table 1
Melting points and melting enthalpies of $Ce(PO_3)_3$ and M^IPO_3 (M^I = Li, Na, K, Rb, Cs, Ag, Tl)

Components	$T_{\mathrm{fus}}^{0(\mathrm{experimental})}$ (K)	$\Delta_{\mathrm{fus}} H_{\mathrm{m}}^{0(\mathrm{experimental})}$ (kJ mol^{-1})	$\Delta_{\mathrm{fus}} H_{\mathrm{m}}^{0(\mathrm{literature})}$ (kJ mol^{-1})
$Ce(PO_3)_3$	1529	75.22	Not found
$LiPO_3$	936	24.20	25.50 [4]; 24.62 [6]
$NaPO_3$	909	23.73	22.20 [4,7]
KPO_3	1084	13.61	10.9 [4]
$RbPO_3$	1079	9.89	11.1 [4,7]
$CsPO_3$	1006	11.52	10.1 [4,7]
$AgPO_3$	767	11.84	11.7 [4,7]
$TlPO_3$	711	14.45[a]	17.2[a] [4]

[a] The value given is the melting enthalpy of the α-phase.

2. Experimental

The melting enthalpies of monovalent metal polyphosphates and cerium polyphosphate were determined using a Setaram DTA 92 apparatus coupled to a calculator allowing, through an appropriate program, integration of area of the different thermal effects. The melting enthalpies of K_2SO_4 and CaF_2 [5] were utilized to calibrate the apparatus. Samples of 0.02 g, in a platinum crucibles, were used and the heating rate of the furnace was 5 K min^{-1}. This apparatus was used to measure the melting points of the above samples. The onset temperature in DTA curve was considered. Pt/Pt–Rh thermocouple was used at temperature higher than 1273 K, below this temperature, a Pt/Platinel thermocouple was sufficient.

Table 2
Thermal effects in the $LiPO_3$–$Ce(PO_3)_3$ system

x[a]	T_F[b] (K)	T_E[c] (K)	T_P[d] (K)
0	936		
5	1028	925	
10	1113	923	
15	1163	920	
20	1198	923	
25	1223	923	
30	1243	922	
35	1253	923	1255
40	1283	916	1255
50	1348		1253
60	1403		1251
70	1438		1248
80	1478		1240
100	1529		

[a] Mole fraction of $Ce(PO_3)_3$.
[b] Liquidus temperature.
[c] Eutectic temperature.
[d] Peritectic temperature.

Table 3
Thermal effects in the KPO_3–$Ce(PO_3)_3$ system

x[a]	T_F[b] (K)	T_t[c] (K)	T_E[d] (K)	T_{P1}[e] (K)	T_{P2}[e] (K)
0	1084	725			
2	1073	727	968		
5	1049	725	971		
8	1025	725	973		
10	1010	725	972		
15	1004	725	971		
20	1062	722	971	1016	
25	1098	722	968	1020	
30	1141	722	960	1014	
33	1146			1014	
35	1151			1013	
40	1246			1004	1160
45	1286			1000	1158
50	1320				1155
55	1346				1153
60	1373				1150
65	1399				1148
70	1417				1146
75	1441				1142
80	1462				1138
85	1480				1134
90	1499				1130
100	1529				

[a] Mole fraction of $Ce(PO_3)_3$.
[b] Liquidus temperature.
[c] Phase transformation temperature of KPO_3.
[d] Eutectic temperature.
[e] Peritectic temperature.

Table 4
Thermal effects in the $NaPO_3$–$Ce(PO_3)_3$ system

x[a]	T_{F}[b] (K)	T_{E}[c] (K)	T_{P}[d] (K)
0	909		
2	903	900	
5	897	902	
8	973	900	
10	1011	897	
13	1044	899	
18	1084	898	
25	1130	897	
30	1173	895	1138
33	1211	892	1140
43	1292	884	1143
50	1320		1138
58	1373		1138
65	1415		1138
75	1449		1136
85	1487		1135
100	1529		

[a] Mole fraction of $Ce(PO_3)_3$.
[b] Liquidus temperature.
[c] Eutectic temperature.
[d] Peritectic temperature.

Table 5
Thermal effects in the $RbPO_3$–$Ce(PO_3)_3$ system

x[a]	T_{F}[b] (K)	T_{t}[c] (K)	T_{E}[d] (K)	T_{P1}[e] (K)	T_{P2}[e] (K)
0	1079	673			
5	1034	668	943		
10	984	677	950		
15	967	673	948		
20	1056	673	946	974	
25	1106	669	938	990	
30	1139	661	930	983	
33	1148			985	
35	1164			983	
40	1223			976	1175
45	1267				1173
50	1295				1171
60	1373				1166
70	1428				1161
80	1478				1155
100	1529				

[a] Mole fraction of $Ce(PO_3)_3$.
[b] Liquidus temperature.
[c] Phase transformation temperature of $RbPO_3$.
[d] Eutectic temperature.
[e] Peritectic temperature.

Table 6
Thermal effects in the $CsPO_3$–$Ce(PO_3)_3$ system

x[a]	T_{F}[b] (K)	T_{t}[c] (K)	T_{E}[d] (K)	T_{P1}[e] (K)	T_{P2}[e] (K)
0	1006	768			
5	970	773	933		
10	933	768	930		
15	984	775	925		
20	1028	768	938		
25	1086		935	1054	
30	1145		933	1050	
33	1156			1047	
35	1173			1043	
40	1250			1037	1181
45	1309			1040	1178
50	1339				1178
55	1395				1175
65	1428				1165
80	1484				1158
100	1529				

[a] Mole fraction of $Ce(PO_3)_3$.
[b] Liquidus temperature.
[c] Phase transformation temperature of $CsPO_3$.
[d] Eutectic temperature.
[e] Peritectic temperature.

Table 7
Thermal effects in the $TlPO_3$–$Ce(PO_3)_3$ system

x[a]	T_{F}[b] (K)	T_{t}[c] (K)	T_{E}[d] (K)	T_{P1}[e] (K)	T_{P2}[e] (K)
0	711	690			
5	728	688	704		
10	800	686	710		
15	839	685	704		
20	973	685	696	840	
25	1045	682	696	843	
30	1083	682	690	845	
33	1153			846	1087
35	1173			853	1086
40	1228			843	1083
45	1278			848	1080
50	1328				1078
55	1373				1073
60	1395				1071
70	1439				1067
80	1478				1060
100	1529				

[a] Mole fraction of $Ce(PO_3)_3$.
[b] Liquidus temperature.
[c] Phase transformation temperature of $TlPO_3$.
[d] Eutectic temperature.
[e] Peritectic temperature.

Table 8
Thermal effects in the $AgPO_3$–$Ce(PO_3)_3$ system

x[a]	T_F[b] (K)	T_E[c] (K)	T_P[d] (K)
0	767		
5	989	765	
10	1050	770	
15	1134	758	1064
20	1195	761	1061
25	1231	756	1061
30	1273	751	1061
35	1289	756	1055
40	1314	751	1061
45	1339	751	1061
50	1367		1060
55	1378		1055
65	1411		1045
75	1443		1038
100	1529		

[a] Mole fraction of $Ce(PO_3)_3$.
[b] Liquidus temperature.
[c] Eutectic temperature.
[d] Peritectic temperature.

Table 9
M^IPO_3–$Ce(PO_3)_3$ systems: values of $\sum_i \nu_{i0} \ln(x_i/x_{i0})$

Solid phase	$\sum_i \nu_{i0} \ln(x_i/x_{i0})$
M^IPO_3	$\ln(1-x)$
$M^I_pCe(PO_3)_{3+p}$ $(p = 1, 2)$	$\ln[x(1-x)^p(1+p)^{(1+p)}/p^p]$
$Ce(PO_3)_3$	$\ln(x)$

x, mole fraction of $Ce(PO_3)_3$.

3. Results

3.1. Thermal analysis and calorimetry

The different values of melting points and melting enthalpies of M^IPO_3 and $Ce(PO_3)_3$ are determined by DTA and presented in Table 1. Some values of melting enthalpies given by the literatures [4,6,7] were reported in the same table. The DTA results for the systems M^IPO_3–$Ce(PO_3)_3$ (with M^I = Li, Na, K, Rb, Cs, Ag, Tl) [1] are presented in Tables 2–8. The phase equilibrium diagrams obtained and the liquidus curve recalculated are described in Figs. 1–7.

3.2. *Choice of a model for calculation of solid–liquid equilibria in the M^IPO_3–$Ce(PO_3)_3$ systems*

3.2.1. *Equation for liquidus curves*

Several models have been proposed in the literature [8–10] for the description of phase diagram.

As already stated in a previous publication concerning the critical evaluation of binary systems [4], the models used for description of polyphosphates

Table 10
M^IPO_3–$Ce(PO_3)_3$ systems: liquidus of $Ce(PO_3)_3$

Systems	A (K)	B	C	$\Delta_{fus}H^0_m$ (kJ mol^{-1})	$\Delta C^0_{p,m}$ (J K^{-1} mol^{-1})	$\Delta_{fus}S^0_m$ (J K^{-1} mol^{-1})	T^0_{fus} (K)
$LiPO_3$–$Ce(PO_3)_3$	13028.62	14.67	−116.11	78.22	121.98	51.15	1529
$NaPO_3$–$Ce(PO_3)_3$	10482.78	12.39	−97.69	70.34	102.99	45.99	1529
KPO_3–$Ce(PO_3)_3$	14530.66	14.87	−118.56	68.28	123.65	44.65	1529
$RbPO_3$–$Ce(PO_3)_3$	12798.26	13.51	−107.44	65.37	112.33	42.75	1529
$CsPO_3$–$Ce(PO_3)_3$	31265.94	27.34	−220.91	87.63	227.29	57.30	1529
$AgPO_3$–$Ce(PO_3)_3$	5986.74	10.63	−81.85	85.35	88.367	55.82	1529
$TlPO_3$–$Ce(PO_3)_3$	16690.01	15.59	−132.56	72.16	137.93	47.19	1529

Table 11
M^IPO_3–$Ce(PO_3)_3$ systems: liquidus of M^IPO_3 (M^I = Na, K, Rb, Cs, Tl)

Systems	A (K)	B	C	$\Delta_{fus}H^0_m$ (kJ mol^{-1})	$\Delta C^0_{p,m}$ (J K^{-1} mol^{-1})	$\Delta_{fus}S^0_m$ (J K^{-1} mol^{-1})	T^0_{fus} (K)
$NaPO_3$	−165986.90	−180.16	1409.92	18.24	−1497.85	20.07	909
KPO_3	11183.43	12.08	−94.67	15.81	100.35	14.58	1084
$RbPO_3$	2532.67	3.60	−27.50	11.26	29.95	10.43	1079
$CsPO_3$	443.82	1.86	−13.28	11.84	15.44	11.77	1006
$TlPO_3$	2227.31	5.59	−39.83	14.52	46.46	20.42	711

Table 12
M^IPO_3–$Ce(PO_3)_3$ systems: liquidus of $M^I_pCe(PO_3)_{3+p}$ ($p = 1, 2$)

Systems	A (K)	B	C	$\Delta_{fus}H^0_m$ (kJ mol^{-1})	$\Delta C^0_{p,m}$ (J K^{-1} mol^{-1})	$\Delta_{fus}S^0_m$ (J K^{-1} mol^{-1})	T^0_{fus} (K)
$LiCe(PO_3)_4$	−759.85	7.24	−51.15	82.66	60.21	65.19	1268
$NaCe(PO_3)_4$	3900.88	10.13	−74.92	66.69	84.19	56.64	1177
$KCe(PO_3)_4$	−1897.19	1.84	−11.42	33.98	15.27	28.51	1191
$RbCe(PO_3)_4$	4169.07	6.62	−50.42	31.73	55.03	26.30	1206
$CsCe(PO_3)_4$	10721.20	11.85	−93.01	30.60	98.55	25.18	1215
$AgCe(PO_3)_4$	28545.51	38.94	−299.10	130.70	323.75	114.98	1136
$TlCe(PO_3)_4$	8204.18	10.46	−80.82	31.48	86.94	27.45	1146
$K_2Ce(PO_3)_5$	127315.30	133.48	−1049.72	95.67	1109.78	91.99	1040
$Rb_2Ce(PO_3)_5$	−4519.22	−0.32	6.54	34.83	−2.63	33.44	1041
$Cs_2Ce(PO_3)_5$	−30606.47	−26.52	213.59	13.40	−220.52	12.25	1093
$Tl_2Ce(PO_3)_5$	3393.60	10.26	−73.41	47.09	85.27	53.32	883

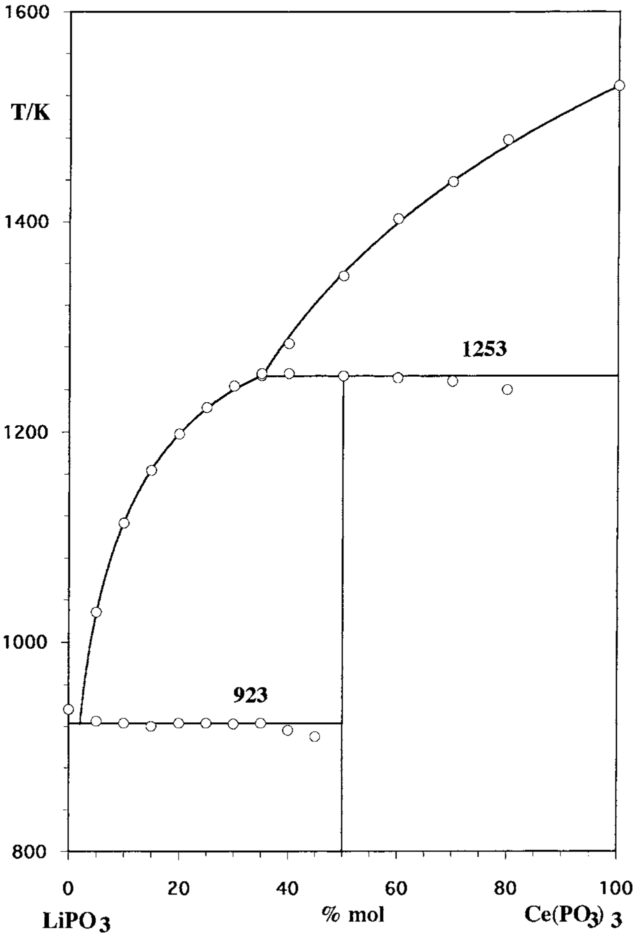

Fig. 1. Equilibrium diagram of the $LiPO_3$–$Ce(PO_3)_3$ system: (—) liquidus curve recalculated; (○) experimental points.

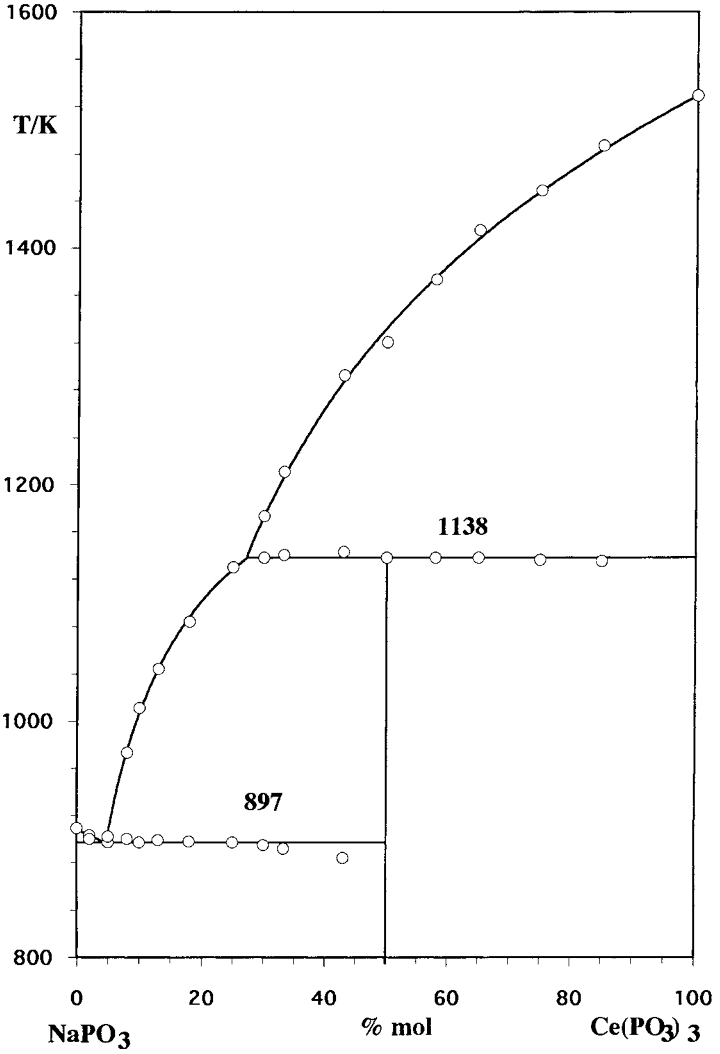

Fig. 2. Equilibrium diagram of the $NaPO_3$–$Ce(PO_3)_3$ system: (—) liquidus curve recalculated; (○) experimental points.

systems must comply with several constraints:

- the solid phases (M^IPO_3, $Ce(PO_3)_3$, $M^ICe(PO_3)_4$, $M^I_2Ce(PO_3)_5$) are stoichiometric;
- the fitting equations of liquidus curves must never be in contradiction with thermodynamic laws;
- the model can be extended to systems presenting an associate liquid phase.

The selected model presented in a previous paper [4] was re-examined [11] and applied to molten salt systems. The analytical expression perfectly describes the liquidus of all solid phases of M^IPO_3–$Ce(PO_3)_3$ systems and has the general formula:

$$\sum_i \nu_{i0} \ln\left(\frac{x_i}{x_{i0}}\right) = \frac{A}{T} + B \ln T + C \qquad (1)$$

where ν_{i0} is the stoichiometry of the species i in the solid, x_{i0} and x_i are the mole fractions of species i in the solid and the liquid phases, respectively. A, B and C are constants and can be calculated by a least

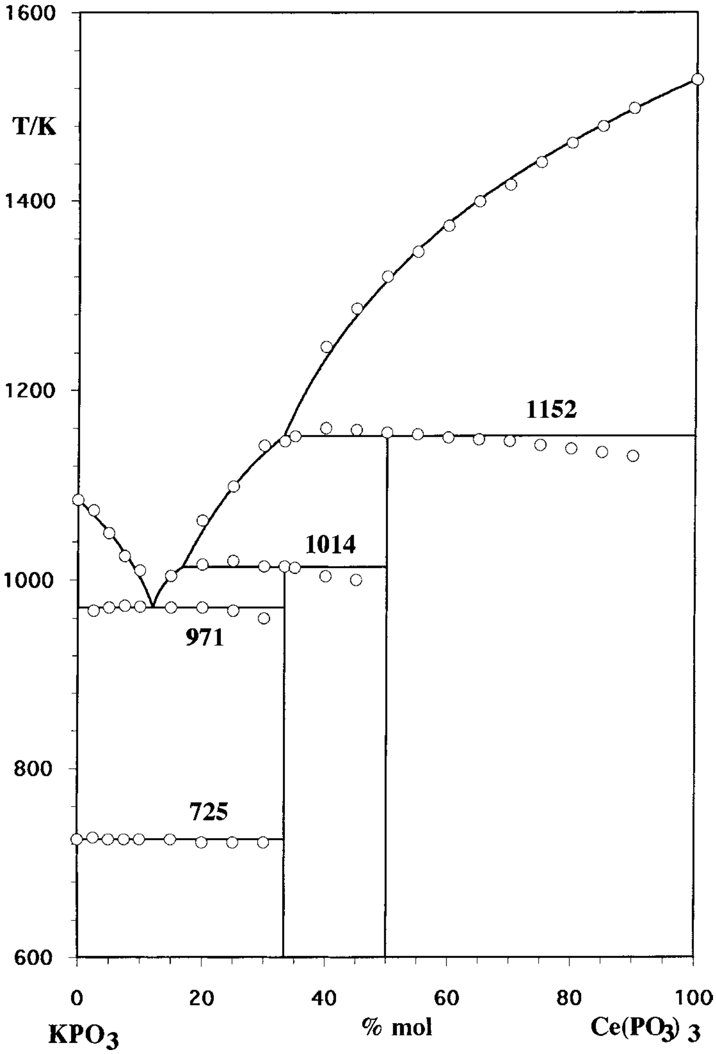

Fig. 3. Equilibrium diagram of the KPO_3–$Ce(PO_3)_3$ system: (—) liquidus curve recalculated; (○) experimental points.

squares method. These constants may be expressed by the relations:

$$A = \frac{(\Delta C^0_{p,\mathrm{m}} T^0_{\mathrm{fus}} - \Delta_{\mathrm{fus}} H^0_{\mathrm{m}})}{R} - \alpha \qquad (2)$$

$$B = \frac{\Delta C^0_{p,\mathrm{m}}}{R} - \beta \qquad (3)$$

$$C = \frac{\Delta_{\mathrm{fus}} H^0_{\mathrm{m}}}{R T^0_{\mathrm{fus}}} - \frac{\Delta C^0_{p,\mathrm{m}}(1 + \ln T^0_{\mathrm{fus}})}{R} - \gamma \qquad (4)$$

where R is the perfect gas constant and T^0_{fus} the stable or metastable melting point of the pure substance. $\Delta_{\mathrm{fus}} H^0_{\mathrm{m}}$ and $\Delta C^0_{p,\mathrm{m}}$ are the variations of heat enthalpy and heat capacity of the pure substance at the fusion, respectively.

Coefficients α, β and γ may be expressed by an equation of the algebraic type:

$$\sum_i \nu_{i0} \ln\left(\frac{\gamma_i}{\gamma_{i0}}\right) = \frac{\alpha}{T} + \beta \ln T + \gamma \qquad (5)$$

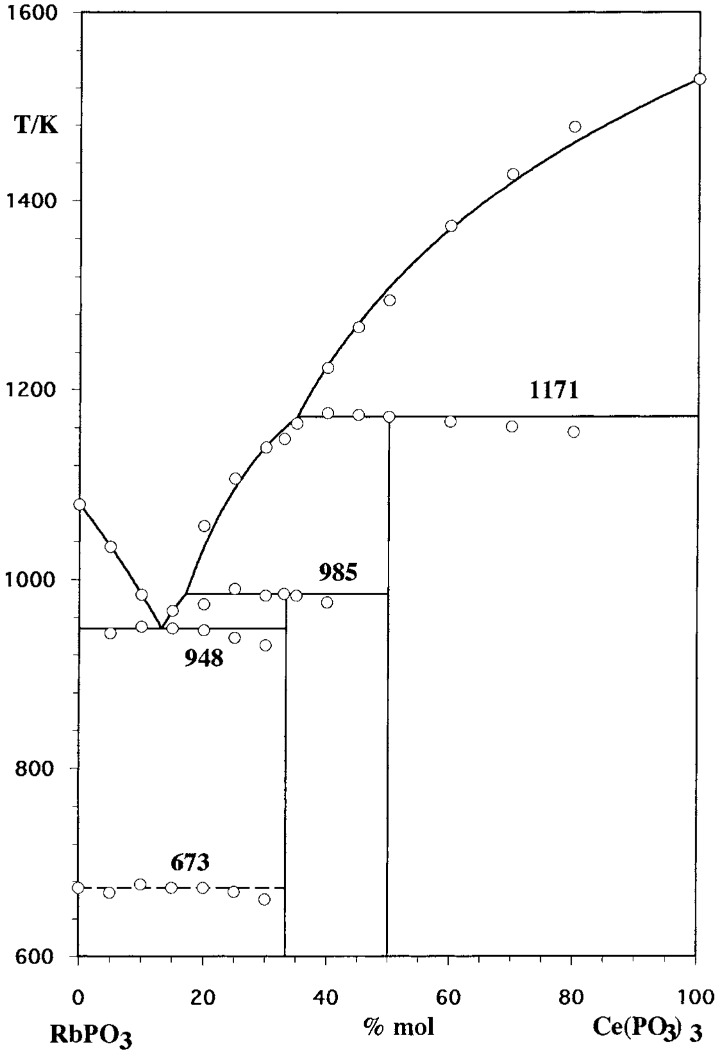

Fig. 4. Equilibrium diagram of the $RbPO_3$–$Ce(PO_3)_3$ system: (—) liquidus curve recalculated; (○) experimental points.

where γ_i and γ_{i0} are the activity coefficients of species i in the liquid and the solid phase, respectively.

The calculation of A, B and C parameters is carried out using the N experimental points (x_j, T_j) and minimizing the following expression:

$$Q = \sum_{j=1}^{N} \left(\left(\sum_i \nu_{i0} \ln \left(\frac{x_i}{x_{i0}} \right) \right) - \left(\frac{A}{T} + B \ln T + C \right) \right)^2 \quad (6)$$

3.2.2. Fitting equation

The first member of Eq. (1) can be easily expressed as a function of the composition of liquid phase. If we assume that the species of the liquid phase are only M^IPO_3 and $Ce(PO_3)_3$, the values of the left side of Eq. (1) for the solid phases of the M^IPO_3–$Ce(PO_3)_3$ systems are given in Table 9, where x is the mole fraction of $Ce(PO_3)_3$ in the liquid phase.

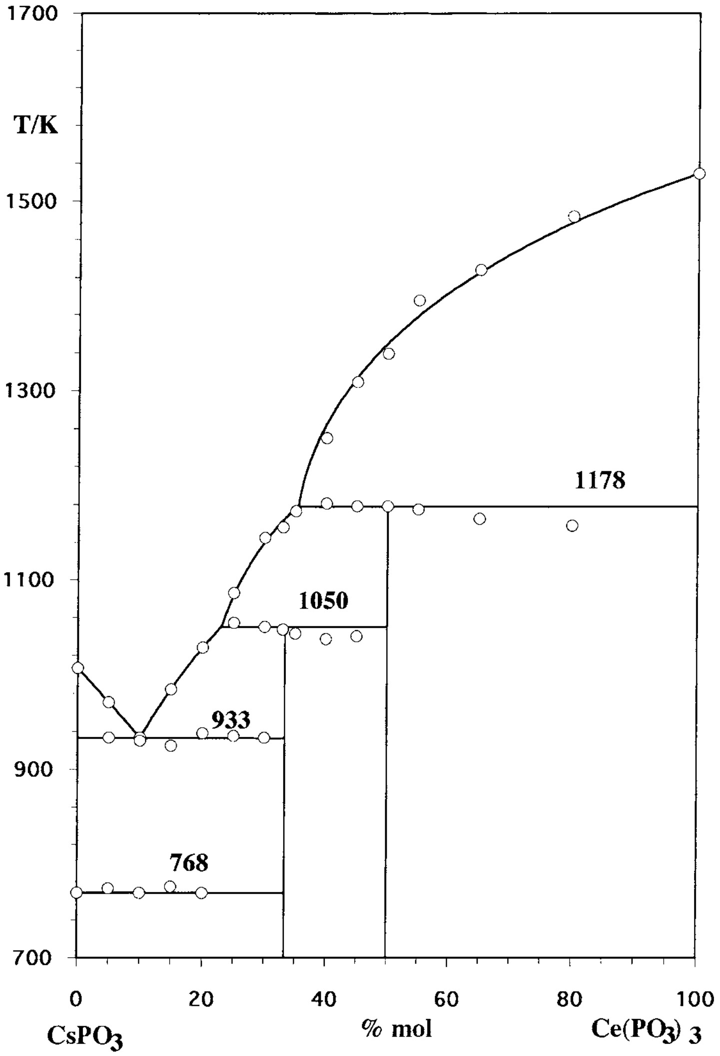

Fig. 5. Equilibrium diagram of the $CsPO_3$–$Ce(PO_3)_3$ system: (—) liquidus curve recalculated; (○) experimental points.

4. Discussion

4.1. Analysis of the liquidus curves

The parameters of the liquidus equation of $Ce(PO_3)_3$ were calculated for each system. They are given in Table 10.

In general, the liquidus curves of M^IPO_3 were defined by a small number of experimental values. Because the melting point T^0_{fus} of pure solids is more precisely known than the determined solubility values, the liquidus curves must pass through these points. The parameters A, B and C of the different M^IPO_3 liquidus equations are presented in Table 11.

The stoichiometry of the intermediate binary compounds found in the different systems corresponds to the formula $M^I_p\,Ce(PO_3)_{3+p}$ with $p = 1$ or 2.

All these phases undergo a peritectic decomposition. Their metastable melting points were calculated and are presented in Table 12 with the parameters A, B and C.

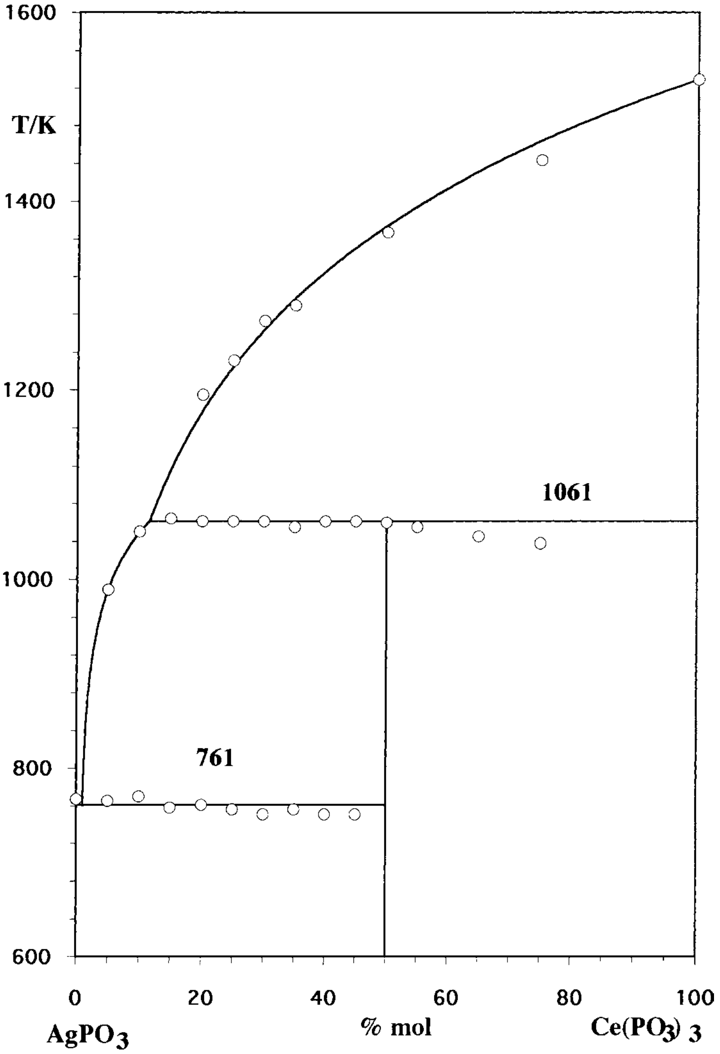

Fig. 6. Equilibrium diagram of the $AgPO_3$–$Ce(PO_3)_3$ system: (—) liquidus curve recalculated; (○) experimental points.

4.2. Thermodynamic exploitation of liquidus curves

When the liquidus equation is known, the thermodynamic functions characteristic of the stable or metastable fusion can be calculated for the ideal solution ($\alpha = \beta = \gamma = 0$) from Eqs. (2)–(4).

The values of the melting enthalpy of cerium polyphosphate obtained in the different systems are coherent (Table 10) and in good agreement with experimental data.

All the intermediate phases decompose peritectically on heating and their fusion was not studied further by calorimetry. The thermodynamic functions of fusion were calculated at the metastable melting point. The results are displayed in Table 12. These values are given only as an indication, since they are calculated on the assumption that the solution is ideal and the liquid phase is only formed by M^IPO_3 and $Ce(PO_3)_3$.

The liquidus study of the M^IPO_3 polyphosphates was limited to the sodium, potassium, rubidium and cesium salts, whose experimental liquidus curves were

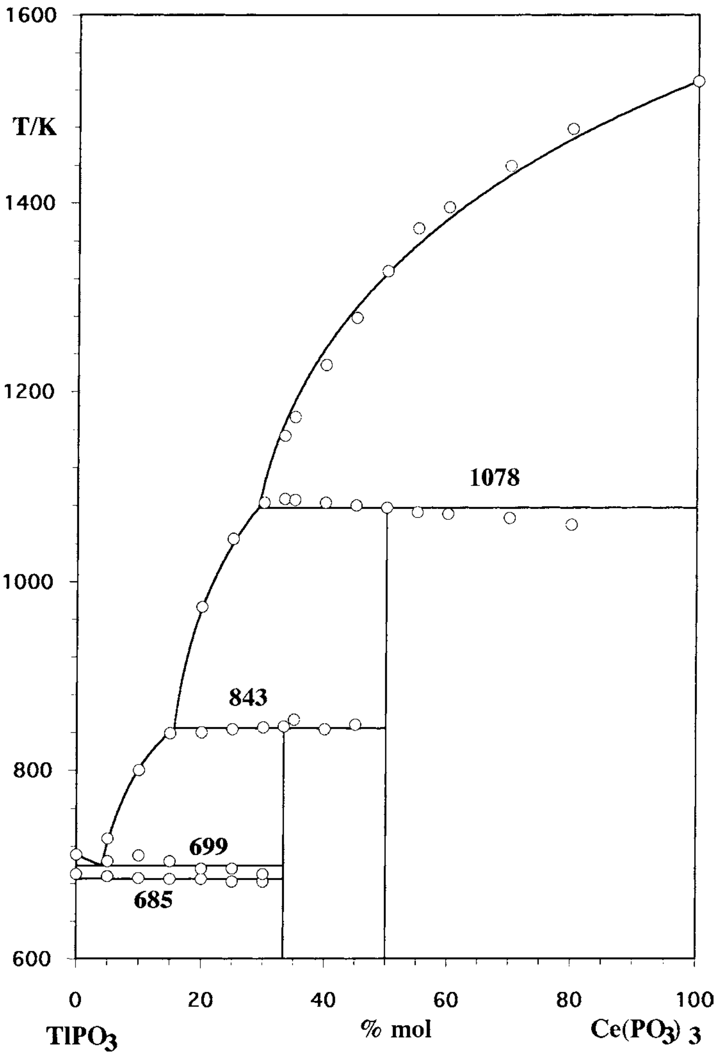

Fig. 7. Equilibrium diagram of the $TlPO_3$–$Ce(PO_3)_3$ system: (—) liquidus curve recalculated; (○) experimental points.

sufficiently well defined to allow a thermodynamic exploitation. Given the precision and the number of experimental determinations, the calculated values of the enthalpy of fusion (Table 11) agree with the experimental ones and with results given by the previous thermodynamic study of M^IPO_3–$Pr(PO_3)_3$ systems [7].

5. Conclusion

A semi-empirical equation of the liquidus curve, already established in the water–salt binary systems was applied with success to salt-salt systems: M^IPO_3–$Ce(PO_3)_3$ (with M^I = Li, Na, K, Rb, Cs, Ag, Tl).

This equation is useful for an intermediate or limit phase in the complete range of temperatures and compositions. The analytical expression obtained perfectly describes the experimental liquidus curves of all the solid phases in the M^IPO_3–$Ce(PO_3)_3$ systems. Moreover, the thermodynamic function characteristic of the fusion was calculated with a simplified hypothesis for all the solid phases whose experimental liquidus curves have been determined. Comparison of the measured and calculated values of heat enthalpies of $M^{I}PO_3$ and $Ce(PO_3)_3$ can be considered to be in concordance.

References

[1] M. Rzaigui, Thèse, Tunisia, 1983.

[2] J.J. Counioux, R. Tenu, J. Chim. Phys. 78 (1981) 815; R. Tenu, J.J. Counioux, J. Chim. Phys. 78 (1981) 823.

[3] J.J. Counioux, R. Tenu, J. Chim. Phys. 82 (1985) 43.

[4] D. Ben Hassen, N. Kbir Ariguib, M. Trabelsi, R. Tenu, J.J. Counioux, Thermochim. Acta 116 (1987) 85–100.

[5] J. Saurel, J. Debaene, J.J. Baron, Technique de l'ingénieur (Constants) (Paris) K2 (2–4) (1989) K600.

[6] K.S. Pitzer, J. Phys. Chem. 77 (1973) 268–277.

[7] J.L. Cruz, Revue de l'Institut Français du pétrole 32 (1977) 393.

[8] J. Wisniak, A. Tamir, Mixing and Excess Thermodynamic Properties, Elsevier, Amsterdam, 1978.

[9] M.T. Cohen-Adad, R. Cohen-Adad, D. Ben Hassen-Chehimi, in: M.A. Cuevas-Diarte, L. Li Tamarit, E. Estop (Eds.), JEEP XIX, Barcelona, 1993, p. 1, ISBN 84-604-5729-X.

[10] D. Ben Hassen-Chehimi, N. Kbir-Ariguib, M. Trabelsi-Ayedi, J. Therm. Anal. 53 (1998) 871–882.

[11] M. Elmokhtar, H. Said, L. Michel, M. Ganteaume, R. Castanet, J. Therm. Anal. 44 (1995) 1251–1259.